British Journal of Pharmacology

DOI:10.1111/bph.12165
www.brjpharmacol.org

RESEARCH PAPER

# Loss of constitutive activity is correlated with increased thermostability of the human adenosine $A_{2A}$ receptor

Nicolas Bertheleme[1], Shweta Singh[1], Simon J Dowell[2], Julia Hubbard[3] and Bernadette Byrne[1]

[1]*Division of Molecular Biosciences, Imperial College London, London, UK,* [2]*Department of Biological Reagent and Assay Development, GlaxoSmithKline, Stevenage, UK, and* [3]*Department of Computational and Structural Chemistry, GlaxoSmithKline, Stevenage, UK*

**Correspondence**
Dr Bernadette Byrne, Division of Molecular Biosciences, Imperial College London, London SW7 2AZ, UK. E-mail: b.byrne@imperial.ac.uk

**Keywords**
G-protein-coupled receptors; adenosine $A_{2A}$ receptor; thermostability; constitutive activity; agonist-induced activity; structure

**Received**
2 October 2012
**Revised**
12 February 2013
**Accepted**
19 February 2013

## BACKGROUND AND PURPOSE

Thermostabilization by mutagenesis is one method which has facilitated the determination of high-resolution structures of the adenosine $A_{2A}$ receptor ($A_{2A}R$). Sets of mutations were identified, which both thermostabilized the receptor and resulted in preferential agonist (Rag23 mutant) or antagonist (Rant5 and Rant21) binding forms as assessed by radioligand binding analysis. While the ligand-binding profiles of these mutants are known, the effects these mutations have on receptor activation and downstream signalling are less well characterized.

## EXPERIMENTAL APPROACH

Here we have investigated the effects of the thermostabilizing mutations on receptor activation using a yeast cell growth assay. The assay employs an engineered *Saccharomyces cerevisiae*, MMY24, which couples receptor activation to cell growth.

## KEY RESULTS

Analysis of the receptor activation profile revealed that the wild-type (WT) $A_{2A}R$ had considerable constitutive activity. In contrast, the Rag23, Rant5 and Rant21 thermostabilized mutants all exhibited no constitutive activity. While the preferentially antagonist-binding mutants Rant5 and Rant21 showed a complete lack of agonist-induced activity, the Rag23 mutant showed high levels of agonist-induced receptor activity. Further analysis using a mutant intermediate between Rag23 and WT indicated that the loss of constitutive activity observed in the agonist responsive mutants was not due to reduced G-protein coupling.

## CONCLUSIONS AND IMPLICATIONS

The loss of constitutive activity may be an important feature of these thermostabilized GPCRs. In addition, the constitutively active and agonist-induced active conformations of the $A_{2A}R$ are distinct.

### Abbreviations

3AT, 3-aminotriazole; $A_{2A}R$, adenosine $A_{2A}$ receptor; FDGlu, fluorescein-Di-β-D-glucopyranoside; ICL3, third intracellular loop; WT, wild-type; YNB, yeast nitrogen base

## Introduction

GPCRs form a large family of cell surface receptors mediating cellular responses to a wide range of external stimuli including hormones, neurotransmitters, odourants and nucleotides (Gloriam *et al.*, 2007). GPCRs have a highly conserved architecture; however, the sequence homology is low particularly in the extracellular loop regions, most likely as a result of the

requirement for recognition and binding of a wide range of ligands (Peeters *et al.*, 2011). Binding of a cognate ligand to the specific binding site of the receptor initiates a conformational change allowing recruitment and activation of the receptor specific G-protein, which in turn initiates an intracellular signalling cascade. GPCRs exhibit significant conformational flexibility reflecting a number of functional states (Kobilka and Deupi, 2007). Agonists cause full activation of the receptor; however, partial agonists induce submaximal activation of the G-protein even at saturating concentrations. In addition, it is well documented that many GPCRs exhibit constitutive, agonist-independent activity (Milligan *et al.*, 1995; Strange, 2002; Gloriam *et al.*, 2007). Antagonists inhibit ligand binding but do not affect constitutive activity, while inverse agonists decrease constitutive activity.

There have been marked advances in our understanding of the mechanism of action of GPCRs in the last 4 years or so as a result of the high-resolution structures of several receptors in a number of different states. Significant progress has been made through the development of GPCR fusion proteins, where a T4 lysozyme replaces the conformationally dynamic third intracellular loop (ICL3), for example (Cherezov *et al.*, 2007; Jaakola *et al.*, 2008; Chien *et al.*, 2010; Wu *et al.*, 2010; 2012; Shimamura *et al.*, 2011; Xu *et al.*, 2011; Granier *et al.*, 2012; Thompson *et al.*, 2012). In each case, the insertion was essential for obtaining well-diffracting crystals with the T4 lysozyme mediating the crystal contacts. The solved structures have provided unprecedented detail of the binding sites of the individual receptors, highlighting key receptor-specific differences and the first definitive insight into the conformational changes involved in switching between agonist- and antagonist-bound states. One recent addition to the structural gallery is the complex of the $\beta_2$ adrenoceptor together with the heterotrimeric $G_s$, which revealed conformational changes in both the receptor and G-protein occurring upon association (Rasmussen *et al.*, 2011).

An alternative approach involves alanine-scanning mutagenesis coupled with radioligand-binding analysis after heating the receptor in order to identify mutants with retained function but increased thermostability. This approach has been applied to three receptors to date, the turkey $\beta_1$ adrenoceptor (Serrano-Vega *et al.*, 2008), the adenosine $A_{2A}$ receptor ($A_{2A}R$) (Magnani *et al.*, 2008) and the neurotensin 1 receptor (Shibata *et al.*, 2009). In each case, combinations of a small number of point mutations resulted in receptor forms with significantly increased thermostability and greater stability in small chain detergents compared with the WT. The thermostabilized turkey $\beta_1$ adrenoceptor was subsequently successfully crystallized, and a number of high-resolution structures solved (Warne *et al.*, 2008; 2011). An agonist-bound structure of thermostabilized mutant $A_{2A}R$ was also recently solved (Lebon *et al.*, 2011). One issue with this method is that while the thermostabilizing mutations are transferable between highly homologous receptors, e.g. the $\beta_1$ and the $\beta_2$ adrenoceptors (Serrano-Vega and Tate, 2009), it has so far not been possible to transfer between more distantly related receptors and, thus, a complete alanine scan must be completed for each receptor. While these structures have significantly advanced our understanding of the structure–function relationships of GPCRs, they are essentially static snapshots of the receptors and lack information on the dynamic changes of these molecules. Also, the structures have generally been of receptors highly engineered either through the insertion of T4 lysozyme in the ICL3, or by the introduction of stabilizing mutations. The effect of these modifications on the receptor-signalling function has not typically been described. Indeed, the replacement of the ICL3 with T4 lysozyme in the vast majority of the GPCR structures determined has prevented characterization of signalling function.

In this study, we aimed to explore the molecular basis of stabilization of the $A_{2A}R$, one of a group of receptors responsible for mediating cellular responses to the purine nucleoside, adenosine. We used previously described thermostable mutants with a preference for either the agonist- (Rag23) or antagonist-binding conformations (Rant5, Rant21) (Magnani *et al.*, 2008) and a yeast cell growth assay, which can distinguish between constitutive and agonist-induced receptor activation. The results presented in this manuscript provide the first report of how these modifications affect receptor activation and reveal that in the case of these mutant receptors, inhibition of constitutive activity is correlated with receptor thermostabilization.

## Methods

### *Materials*

Yeast nitrogen base (YNB) and yeast extract were purchased from Difco (Franklin Lakes, NJ, USA). Peptone, L-histidine, EDTA, EGTA, BSA, Folin-Ciocalteau reagent, amino acids, 3-aminotriazole (3AT) and theophylline were obtained from Sigma-Aldrich (Gillingham, UK), and dimethyl sulfoxide from Acros Organics (Geel, Belgium). Scintillation cocktail (Ultima Gold MV) and [$^3$H]NECA were obtained from PerkinElmer (Cambridge, UK). [$^3$H]ZM241385 was purchased from American Radiolabelled Chemicals Inc. (Stevenage, UK) while ZM241385 and NECA were obtained from Tocris (Abingdon, UK). GF/B filters were purchased from Whatman (Maidstone, UK). The Lightning Quikchange site-directed mutagenesis kit was obtained from Stratagene/Agilent (Stockport, UK). Fluorescein-Di-β-D-glucopyranoside (FDGlu) was purchased from Invitrogen (Paisley, UK).

### *Construct generation and mutagenesis*

Rant5, Rant21 and Rag23 $A_{2A}R$ mutants were obtained from GeneArt (Regensburg, Germany). All synthetic genes encoded the full-length $A_{2A}R$ gene and contained a FLAG tag at the N terminus. The genes were cloned into the pDDGFP *Saccharomyces cerevisiae* expression plasmid (Newstead *et al.*, 2007). The construct comprises the receptor gene upstream of the gene coding for GFP-His8. The pDDGFP plasmids were then digested using BamHI and HindIII, which excised the complete gene coding for the $A_{2A}R$ + GFP-His8 fusion proteins. These genes were then ligated into the integrating p306GPD (Dowell and Brown, 2009) vector. The wild-type (WT) $A_{2A}R$ and intermediate mutants were generated from either the Rant5 or Rag23 synthetic genes by site-directed mutagenesis using the QuickChange Lightning Site-Directed Mutagenesis kit and the primers detailed in Supporting Information Table S1. The single and double mutants intermediate between Rant5 and WT are indicated by the mutant name.

The Rag23-A208L mutant was generated by mutating the A208 of Rag23 back to the WT Leu residue.

## Expression

All the $A_{2A}R$ constructs were fusions with a C-terminal GFP-8His tag in the p306GPD vector, transformed using the lithium-acetate procedure (Gietz and Schiestl, 2007) and chromosomally integrated at the *ura3* locus in the MMY24 (*MAT*a *fus1*::*FUS1-HIS3 LEU2*::*FUS1-lacZ far1 sst2 ste2 gpa1*::*ADE2 his3 ura3 trp1* Gpa1p/Gαi3) yeast strain (Dowell and Brown, 2009). The WT and Rag23-A208L constructs were also transformed into the MMY11 (*MAT*a *fus1*::*FUS1-HIS3 LEU2*::*FUS1-lacZ far1 sst2 ste2 gpa1*::*ADE2 his3 ura3 trp1*) yeast strain. Estimation of the expression levels for all the constructs using GFP as previously described (Newstead *et al.*, 2007) gave values between 0.7 and 1.6 mg·mL$^{-1}$ (Supporting Information Table S2).

## Yeast growth assay

A yeast cell growth assay was used to analyse the G-protein coupling and activation of the different $A_{2A}R$ constructs. This assay utilizes a modified *S. cerevisiae* strain, MMY24 (Brown *et al.*, 2003), which has been genetically engineered to allow functional characterization of heterologous GPCRs. In this strain, the gene encoding for Ste2p, the only yeast GPCR capable of coupling to this pathway in a haploid cell, was deleted and a chimaeric Gα subunit was introduced in which the five C-terminal amino acids of the yeast Gα protein Gpa1p were replaced with the corresponding residues from mammalian $G\alpha_{i3}$ (Brown *et al.*, 2003). Receptor activation induces a reporter gene (*FUS1-HIS3*) in which *HIS3*, encoding the biosynthetic enzyme imidazoleglycerol-phosphate dehydratase, is under control of the pheromone-responsive *FUS1* promoter. Activation of the pathway by GPCR agonism allows the yeast to grow in media lacking histidine. Hence, growth of the cells in the absence of histidine but the presence of receptor specific agonist provides a measure of receptor activation and signalling. Growth of the cells is measured by changes in the levels of fluorescein, the product of the reaction between FDGlu and exoglucanase, an endogenous yeast enzyme secreted from dividing cells (Dowell and Brown, 2009). The mutants expressed in MMY24 were inoculated into –URA media (6.7% YNB, 2% D-glucose, 1.26 g·L$^{-1}$ amino acid supplement [23.53 mg of L-arginine (HCl), 117.6 mg of L-aspartic acid, 117.6 mg of glutamic acid (monosodium), 35.29 mg of L-lysine, 23.53 mg of L-methionine, 58.82 mg of L-phenylalanine, 441.2 mg of L-serine, 235.3 mg of L-threonine, 35.29 mg of L-tyrosine and 176.5 mg of L-valine]) supplemented with histidine to a final concentration of 20 mg·L$^{-1}$, and cultured overnight at 30°C. The cultures obtained were diluted into –URA media supplemented with 26.1 mM $Na_2HPO_4{\cdot}7H_2O$, 21.1 mM $NaH_2PO_4$, pH 7.0 to an $OD_{600}$ of 0.02. The assay mix was supplemented with 3AT, to a final concentration of 5 mM. 3AT is an inhibitor of the imidazoleglycerol-phosphate hydratase. This was calibrated to eliminate background activity from the *FUS1-HIS3* reporter in the absence of GPCR, therefore ensuring that the responses obtained are a measure of receptor signalling (Supporting Information Fig. S1). Adenosine deaminase was not added to the assay mix as preliminary experiments demonstrated that this did not make any difference to the receptor activity (data not shown). FDGlu, a substrate of exoglucanase, an endogenous yeast enzyme secreted from dividing cells, was also added to the medium to a final concentration of 20 μM. The product of this reaction is the fluorescent molecule, fluorescein. An increase in fluorescence (excitation wavelength = 485 nm, emission wavelength = 535 nm) is thus a measure of growth of the culture. Different concentrations of agonist (0.17–0.2 mM) were added. The yeast growth was measured by fluorescence measurement using a microplate reader (TECAN Ultra Evolution, Reading, UK) following 23 h incubation at 30°C. $Log_{10}$ [NECA] against fluorescence curves were plotted and fitted to non-linear regression, providing $EC_{50}$ values. Data were analysed using GraphPad Prism 5.0 (GraphPad Software, San Diego, CA, USA).

## Radioligand binding analysis

Yeast membranes were prepared as previously described (Singh *et al.*, 2008). Saturation and competition binding assays were carried out as described previously (Singh *et al.*, 2010). In brief, for saturation assays, membranes expressing the WT or mutant $A_{2A}R$ forms were incubated with [$^3$H]ZM241385 (0.036–20 nM) or [$^3$H]NECA (0.3–300 nM) in binding buffer (20 mM HEPES pH 7.4, 1 mM EDTA, 1 mM EGTA, 0.1% BSA). Non-specific binding was defined in the presence of 10 mM theophylline at each concentration. In separate experiments, the WT and Rag23-A208L membranes from both the MMY11 and MMY24 strains prepared in the absence of NaCl were incubated with [$^3$H] NECA (0.3–300 nM) in an alternative binding buffer (20 mM HEPES pH 7.4, 1 mM EDTA, 1 mM EGTA, 0.1% BSA, 10 mM $MgCl_2$). Non-specific binding was defined in the presence of 10 mM theophylline at each concentration. Assays were performed at least in duplicate in a final volume of 1 mL containing 20 μg of membrane protein in each tube. The reactions were incubated for 3 h at room temperature and receptor-bound radioligand was collected by filtration through Whatman glass micro-fibre GF/C filters. The filters were allowed to soak in 2 mL Ultima GoldTM XE scintillation fluid for at least 6 h before the radioactivity was determined using an LS 6500 Beckman Coulter scintillation counter. Agonist competition binding profiles for the WT and mutant receptor forms were determined by competition-binding assay. About 20 μg of membrane protein containing WT and mutant $A_{2A}R$ was incubated with a fixed concentration of [$^3$H]ZM241385 (2 nM for WT and Rant5 and 21 and 9 nM for Rag23) and varying concentrations of competing NECA (100 μM to 1 nM for WT and Rag23 and 10 mM to 10 nM for Rant5, Rant21 and T88A) or adenosine (10–10 nM), in a final volume of 1 mL binding buffer. Non-specific binding was defined in the presence of 10 mM theophylline. Initiation, incubation and termination procedures were as described for the saturation-binding assay.

# Results

## The thermostabilized Rag23, Rant5 and Rant21 mutants exhibit no constitutive activity

The WT $A_{2A}R$ as well as the Rant 5 (A54L, T88A, V239A), Rant 21 (A54L, T88A, K122A, V239A) and Rag 23 (F79A, A184L,

## Table 1

Ligand binding and activation profiles for the Rag and Rant mutants

| Receptor form | [$^3$H] ZM241385 $K_d$ ± SEM (nM) | NECA $K_i$ ± SEM (μM) | [$^3$H] NECA $K_d$ ± SEM (nM)*[a] +G-protein | [$^3$H] NECA $K_d$ ± SEM (nM)*[a] –G-protein | NECA $EC_{50}$ ± SEM (nM) | Constitutive activity ± SEM (% of max activity of WT) |
|---|---|---|---|---|---|---|
| WT | 0.85 ± 0.08 | 1.01 ± 0.23 | 8.6 ± 3.7 | 123.9 ± 7.1 | 33 ± 7 | 54.8 ± 1.5 |
| Rag23 | 6.32 ± 0.34 | 0.18 ± 0.02 | – | – | 13 ± 1 | 6.1 ± 0.9 |
| Rag23-A208L | 7.49 ± 0.90 | – | 1.6 ± 0.2 | 14.4 ± 1.3 | 31 ± 3 | 3.6 ± 0.2 |
| Rant5 | 0.74 ± 0.05 | 531 ± 300 | – | – | ND | 5.3 ± 0.4 |
| Rant21 | 0.63 ± 0.09 | 247 ± 18 | – | – | ND | 3.5 ± 0.2 |

*$K_d$s for [$^3$H] NECA were obtained for both the WT and the Rag23-A208L mutant.
[a]The WT and Rag23-A208L receptor forms were expressed both in the presence and absence of G-protein in the MMY24 and MMY11 yeast strains respectively.
ND, no detectable activity; –, not determined.

## Table 2

Activation profile of the single and double mutants intermediate between Rant5 and WT $A_{2A}R$

| Receptor form | NECA $EC_{50}$ ± SEM (μM) | Constitutive activity ± SEM (% of max activity of WT) |
|---|---|---|
| WT | 0.033 ± 0.007 | 54.8 ± 1.5 |
| A54L | 0.100 ± 0.007 | 25.0 ± 1.1 |
| T88A | ND | 39.8 ± 2.3 |
| V239A | 3.5 ± 0.2 | 2.5 ± 0.1 |
| A54L + T88A | ND | 46.4 ± 4.5 |
| A54L + V239A | 4.9 ± 0.5 | 2.6 ± 0.1 |
| T88A + V239A | ND | 3.4 ± 0.3 |

ND, no detectable activity.

R199A, L208A, L272A) and intermediate mutants (Tables 1 and 2) were expressed in an engineered *S. cerevisae* strain, MMY24, in which receptor activation is coupled to yeast cell growth. The cells were treated with different concentrations of NECA, ranging from 0.5 to 0.2 mM; and fluorescence measurements were taken following incubation for 23 h at 30°C. The WT receptor exhibits high levels of constitutive activity, observed as cell growth in the absence of any receptor agonist (Figure 1, Table 1). The constitutive activity accounts for more than 50% of the total activity of the WT receptor. It is possible to at least partially inhibit the constitutive activity with inverse agonists (Supporting Information Fig. S2). Addition of the $A_{2A}R$ agonist, NECA, stimulates further activity of the WT receptor in a concentration-dependent manner ($EC_{50}$ = 33 ± 7 nM; Figure 1; Table 1). The Rag23 thermostabilized agonist-conformation mutant shows slightly more potent agonist-dependent receptor activity compared with WT ($EC_{50}$ = 13 ± 1 nM; Figure 1; Table 1). The thermostabilized antagonist-conformation mutants, Rant5 and Rant21, show no agonist-induced receptor activity. In contrast to the WT, Rag23, Rant5 and Rant21 show no constitutive activity (Figure 1, Table 1). Saturation binding analysis of the WT, Rag23, Rant5 and Rant21 mutants revealed that all the receptor forms exhibit high-affinity binding for the antagonist ZM241385. The specific activities of the mutants show that the functional expression level ($B_{max}$; Supporting Information Table S2) of each of the mutants is higher than that of the WT receptor, indicating that the loss of constitutive activity observed is not due to low functional expression. The affinity of the Rag23 for ZM241385, the thermostabilized agonist-binding form, was reduced by an order of magnitude compared with the WT, Rant5 and Rant21 receptor forms (Table 1, Figure 2). This is in agreement with results reported for expression of these receptor forms in *Escherichia coli* (Magnani *et al.*, 2008). However, the precise $K_d$ values obtained in the yeast expression system described here are lower than those reported for the same constructs expressed in *E. coli*. The $K_d$ value for the WT receptor reported here is consistent with that obtained for the $A_{2A}R$ heterologously expressed in *Pichia pastoris* (Singh *et al.*, 2010), *S. cerevisiae* (O'Malley *et al.*, 2007), CHO cells (Uustare *et al.*, 2005) and $A_{2A}R$ present in rat brain tissue (Alexander and Millns, 2001). Competition-binding analysis revealed that while Rag23 bound the agonist NECA with a reduced $K_i$ compared with the WT (Table 1), the Rant5 and Rant21 had dramatically increased $K_i$ values (Table 1, Figure 2). These results are consistent overall with the binding data obtained for the same receptor constructs expressed in *E. coli* (Magnani *et al.*, 2008).

### *T88 has a major role in mediating NECA binding*

Analysis of the mutants intermediate between Rant5 and WT reveals that the A54L mutant has reduced constitutive activity compared with WT. In addition, while this mutant exhibits agonist-dependent receptor activity, it is less sensitive to NECA than the WT receptor or the Rag23 mutant ($EC_{50}$ = 0.10 ± 0.01 μM; Figure 3, Table 2). The V239A mutant shows lower sensitivity to NECA than A54L ($EC_{50}$ = 3.54 ± 0.22 μM; Figure 3, Table 2) and has no detectable constitutive activity, indicating that the V239 residue plays a crucial role in both agonist-induced and constitutive activities. The A54L + V239A mutant shows an almost identical activities profile to

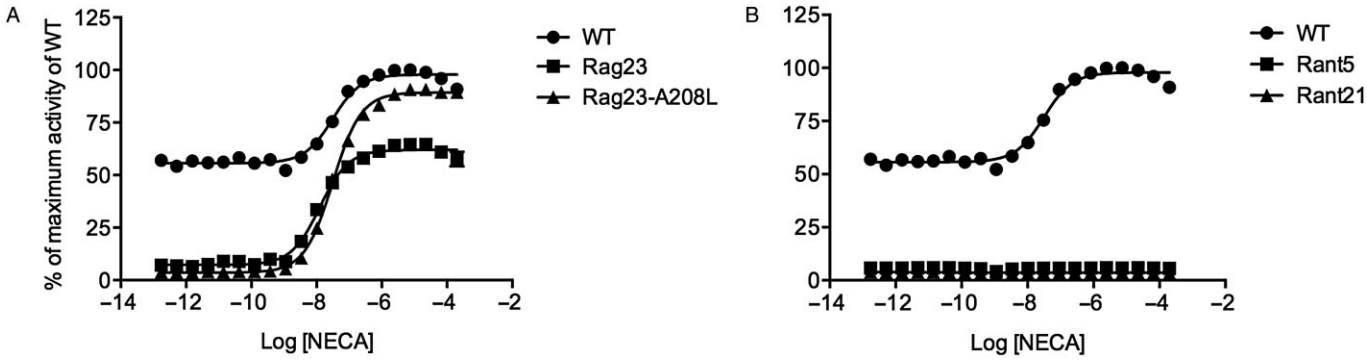


## Figure 1

NECA-induced activity of the thermostabilized mutant $A_{2A}R$ constructs (A) Rag23, Rag23-A208L and (B) Rant5 and Rant21 compared with WT. The maximum response of the WT receptor was taken as 100%, and the response obtained from the cells with no receptor was taken as 0%. The different receptor forms were expressed in the MMY24 *Saccharomyces cerevisiae* strain as constructs in the p306GPD vector. Data points are the average of three different experiments (two different experiments only for the Rag23-A208L mutant) performed in triplicate.

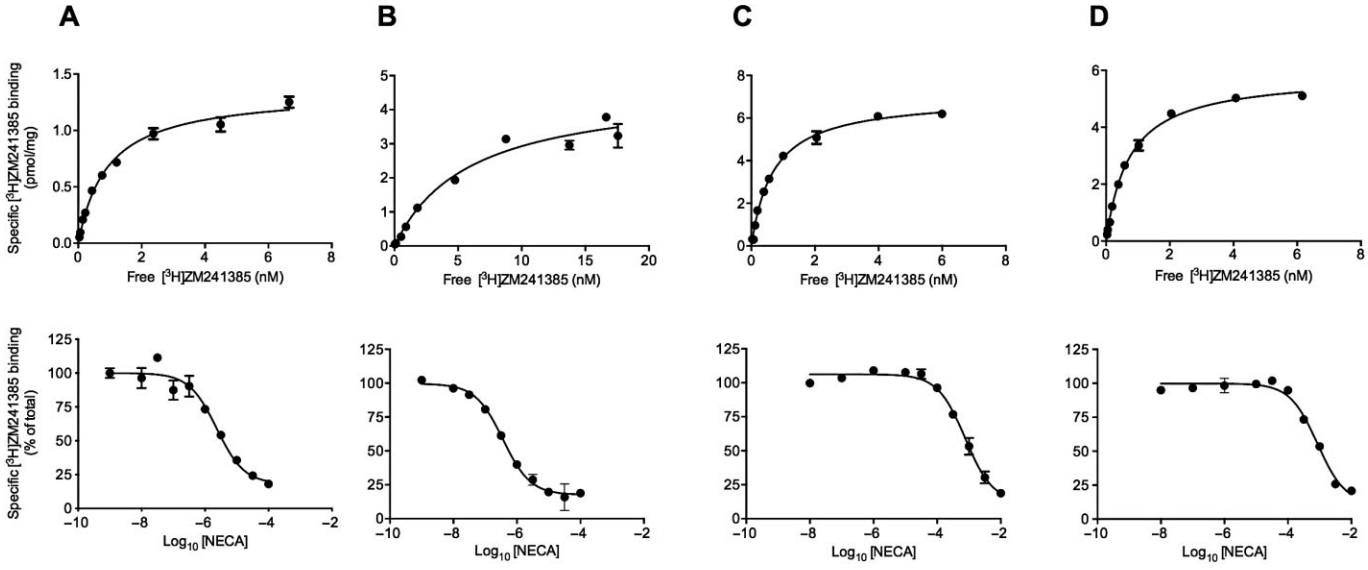


## Figure 2

Saturation binding of [$^3$H] ZM241385 and binding of the low-affinity agonist NECA in competition with [$^3$H]ZM241385 to *Saccharomyces cerevisiae* MMY24 membranes expressing the WT (A), Rag23 (B), Rant5 (C) and Rant21 (D) $A_{2A}R$ constructs. All data are representative of two independent experiments performed in triplicate. $K_d$ values were derived by non-linear regression analysis of the saturation binding data. The competition binding data were fitted to a one binding site model. $K_i$ values were derived from experimentally determined $IC_{50}$ values. Mean data ± SEM are presented in Table 1.

that of the single V239A mutant, while the T88A + V239A mutant shows a complete loss of both constitutive and agonist-dependent activities (Figure 3, Table 2). The T88A mutant also exhibits high levels of constitutive activity, although slightly lower than that observed for the WT, but showed no NECA-induced activity (Figure 4, Table 3). However, stimulation with adenosine induced low but detectable receptor activity (Figure 4, Table 3). The biphasic nature of the T88A adenosine dose–response curve is not due to toxicity of the adenosine (data not shown) but rather to an unexplained pharmacological effect. A similar profile was obtained for ligand binding with the T88A, showing a fivefold reduction in affinity for adenosine and a ~200-fold reduction in affinity for NECA compared with WT (Table 3). Together, these data indicate that the T88A mutant is capable of undergoing the conformational change associated with ligand-mediated activation, but has lost affinity for these ligands.

### *Loss of constitutive activity observed in the Rag23 is not due to the ICL3 mutant L208A*

The fact that Rag23 has no constitutive activity but exhibits NECA-induced activity suggests that the constitutively active

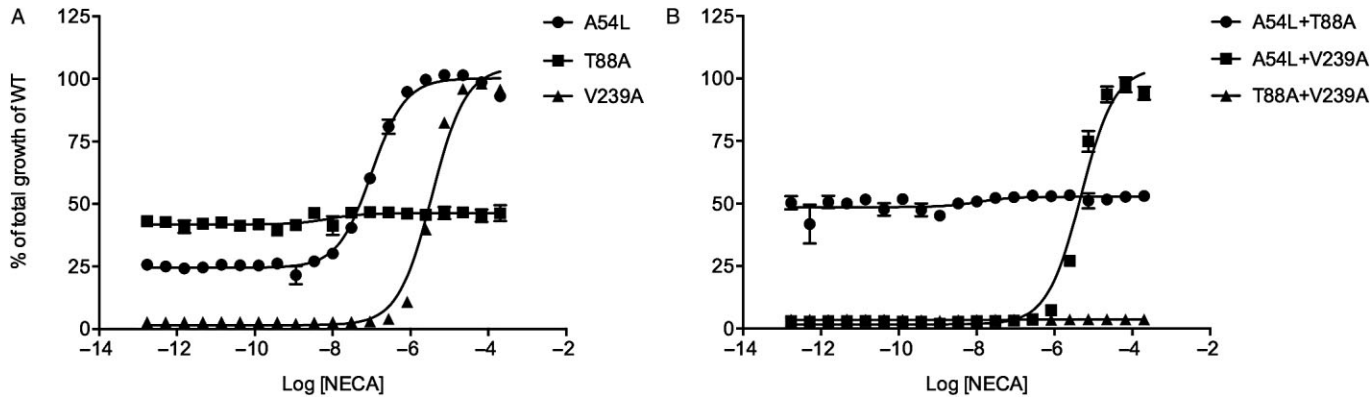


## Figure 3

Functional analysis of the mutants intermediate between WT $A_{2A}R$ and RANT5. The maximum response of the WT receptor was taken as 100% and the response obtained from the cells with no receptor was taken as 0%. The single mutants A54L, T88A, V239A (A) and double mutants A54L +T88A, A54L+V239A and T88A+V239A (B) are shown. The different receptor forms were expressed in the MMY24 *Saccharomyces cerevisae* strain as C-terminal GFP fusion constructs in the p306GPD vector. In each case, the cells were treated with increasing concentrations of the $A_{2A}R$ agonist, NECA. Data points are the average of three different experiments performed in triplicate.

receptor conformation is different from that of the agonist-induced conformation. A closer inspection of the five mutations, which combine to make the Rag23, revealed that one of these, L208A, is located in ICL3. As this region of the receptor is known to have an important role in G-protein coupling, we explored whether this residue is the key in mediating constitutive activity. We generated a mutant intermediate between Rag23 and the WT, Rag23-A208L (F79A, A184L, R199A, L272A), in which Ala208 has been back-mutated into the original Leu. Functional analysis revealed that the Rag23-A208L mutant has no constitutive activity (Figure 1, Table 1), indicating that L208 has little or no role in mediating this activity. However, interestingly, the Rag23-A208L exhibits much higher agonist-induced efficacy than Rag23. Indeed, the Rag23-A208L exhibits close to the maximum WT levels of activity in response to NECA (Figure 1).

### *Differences in levels of constitutive activity are not the result of altered coupling to G-protein*

It is possible that the lack of observed constitutive activity of the Rag23 and Rag23-A208L is the result of altered G-protein coupling for these mutants. The high efficacy of the Rag23-A208L mutant is strongly suggestive that the lack of constitutive activity seen in this mutant is not the result of reduced G-protein coupling. However, in order to investigate this further, we explored the binding of the WT and the Rag23-A208L to [$^3$H] NECA in the presence and absence of the G-protein. This was achieved by also expressing the receptor variants in an alternative yeast strain MMY11 (Olesnicky *et al.*, 1999), genetically identical to MMY24 but lacking the G-protein alpha subunit. It is known that the presence of G-protein increases the affinity of a receptor for agonist by placing the receptor in a high-affinity binding conformation. If G-protein coupling had not been altered in the Rag23-A208L mutant, we would expect to see approximately the same level of reduction in affinity for [$^3$H] NECA in the absence of G-protein for both the mutant and WT receptor forms. The data revealed that for the WT receptor, the absence of G-protein reduced the affinity for NECA by approximately an order of magnitude confirming that Gα affects the affinity state for the ligand. However, the binding affinity for [$^3$H] NECA for Rag23-A208L in the absence of G-protein was also reduced by approximately an order of magnitude compared with the binding affinity in the presence of G-protein (Table 1), indicating that the basis for this mutant's lack of constitutive activity is not simply attributable to failure to bind G-protein.

## Discussion and conclusions

In the yeast cell growth-based assay, a heterologous GPCR is isolated from its native environment and can be studied in combination with a single G-protein species in a completely defined system. This allows simple and rapid assessment of mechanistic aspects of GPCR activation. Here, we profiled the WT $A_{2A}R$ in addition to the previously reported Rag23, Rant5 and Rant21 mutants (Magnani *et al.*, 2008) in order to obtain a greater understanding of the molecular basis of their thermostabilization. We selected experimental conditions in which yeast growth was entirely dependent on GPCR activation and constitutive activity could be clearly observed. The constitutive activity of the $A_{2A}R$ in our experiments compared reasonably to values obtained in HEK293 cells as assessed by cAMP accumulation in which constitutive activity accounted for approximately a third of the maximal CGS21680-induced activity (Klinger *et al.*, 2002). Because the Rag23, Rant5 and Rant21 receptor forms contain a number of point mutations, we also generated various mutant forms intermediate between the Rant5 and the WT. The results of this analysis clearly demonstrate that while Rag23 retains high levels of agonist-induced receptor activity, the Rant mutants exhibit no discernable receptor activation. Although this finding is in broad agreement with the previous study using only

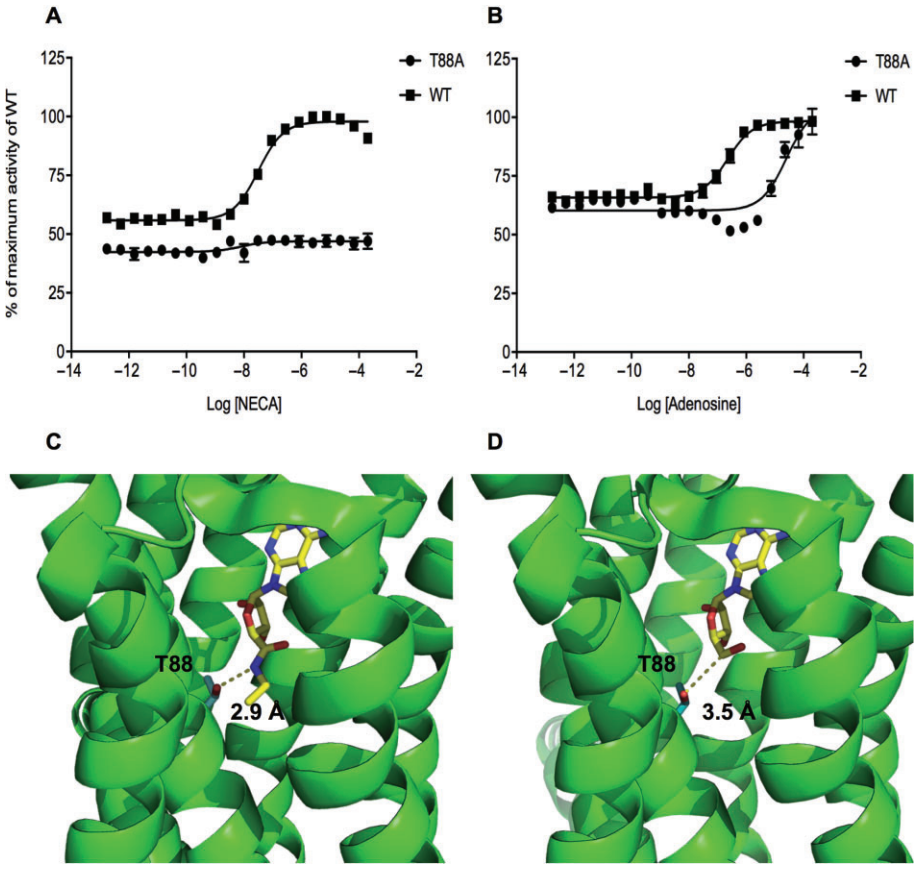


## Figure 4

Activity of the T88A mutant compared with WT $A_{2A}R$ (A, B). The maximum response of the WT receptor was taken as 100% and the response obtained from the cells with no receptor was taken as 0%. The different receptor forms were expressed in the MMY24 *Saccharomyces cerevisiae* strain as constructs in the p306GPD vector. The cells were treated with increasing concentrations of either NECA (A) or adenosine (B). Data points are the average of three different experiments performed in triplicate. Structures of the NECA-bound (C, Pdb accession code 2YDV) and the adenosine-bound (D, PDB accession code 2YDO) $A_{2A}R$ showing the position of the T88 residue relative to the bound ligand. The T88 side chain and the ligands are shown in stick representations. The distances between the hydroxyl group of the T88 and the closest group of the two different ligands are shown by the dotted lines.

## Table 3

Comparison of the NECA and adenosine binding and activation profile of T88A

| | NECA | Adenosine | NECA | Adenosine |
|---|---|---|---|---|
| Receptor form | $K_i$ ± SEM (μM) | $K_i$ ± SEM (μM) | $EC_{50}$ ± SEM (nM) | $EC_{50}$ ± SEM (μM) |
| WT | 1.01 ± 0.23 | 0.36 ± 0.01 | 33 ± 7 | 0.37 ± 0.02 |
| T88A | 187 ± 54 | 2.71 ± 0.06 | ND | 32 ± 3 |

ND, no detectable activity.

radioligand-binding analysis to characterize the mutants (Magnani *et al.*, 2008), here we present for the first time a detailed activation profile for these mutants. One key observation was the total loss of constitutive activity for all three mutant forms. On the basis of these data, it seems likely that the loss of constitutive activity observed for all three mutant receptors is a major contributory factor in their increased thermostability. It should be noted that a recent agonist-bound $A_{2A}R$ structure was obtained of a thermostabilized mutant, GL31 (Lebon *et al.*, 2011). In contrast to the findings presented here, the thermostabilized GL31, which contains a completely different set of point mutations to the Rag23 construct, exhibited WT levels of constitutive activity in a mammalian cell signalling system. Thus, although in the case

of the Rag and Rant mutants thermostability correlates with a loss of constitutive activity, there may be other mechanisms by which thermostability can be achieved without the loss of constitutive activity.

Analysis of the mutants intermediate between WT and Rant5 revealed a clear trend in the characteristics of these mutants with differing degrees of reduced agonist potency and reduced/no constitutive activity. One of the intermediate mutants T88A + V239A has no constitutive activity and no signalling as observed for the Rant5 and Rant21 mutants. Another intermediate mutant A54L + V239A exhibits no constitutive activity and very low but measurable agonist-induced signalling. The Tm for this receptor form in the presence of antagonist was measured as 42°C compared with 46°C for Rant5 and 49°C for Rant21 (Magnani *et al.*, 2008). There is no reported Tm for the T88A + V239A mutant receptor (Magnani *et al.*, 2008) but given the lack of both constitutive and agonist-induced signalling from this construct, it is likely to be similar to the Rant5 and Rant21 mutants. It is clear from the data that the effects of some of the intermediate mutations are additive. For example, the A54L + V239A mutant has no constitutive activity but shows some agonist-induced receptor activity. The A54L + T88A + V239A combination of the Rant5 has no constitutive activity and no detectable agonist-induced receptor activity. It should be noted that the Rant5 does bind NECA with much reduced affinity. The conformation change induced by the mutations is sufficient to prevent receptor activation but still allows low-affinity binding of NECA. Other mutant combinations do not appear to be additive, e.g. A54L + V239A, which has the same receptor activity profile as the V239A-only mutant. It may be that there is a benefit conferred by the A54L that is not detectable by this assay.

Previous research has shown that mutating T88 dramatically reduces both agonist-binding and agonist-induced activities but does not significantly affect antagonist binding (Jiang *et al.*, 1996). The results presented here that support these earlier findings, however, show that the degree to which agonist activity is reduced is dependent on the agonist. NECA failed to induce any receptor activity in the T88A mutant while adenosine induced low but detectable activity. Binding of the two ligands shows the same trend, indicating that the impairment in agonism is due to a reduction of affinity for these agonists. Clues to the precise molecular basis of the difference in the responsiveness of the mutant to the two agonists can be obtained from the recent $A_{2A}R$ structures (Lebon *et al.*, 2011). In the NECA-bound structure, the T88 forms a critical H-bond with the amide group on the ribose ring of the ligand (Figure 4C). In contrast, the structure of the adenosine-bound receptor reveals that T88 is too far away to form a H-bond with the ligand (Figure 4D). Rather, this residue, together with a number of others, appears to play a role in stabilizing the protein via van der Waals interactions. Although in our hands the T88A mutation seems critical for the binding of NECA, the reversion of T88A back to Thr in the thermostabilized $A_{2A}R$ construct that produced the ZM-241385 co-structure did not restore NECA affinity. This could be explained by the presence of other mutations preventing the binding of NECA (Doré *et al.*, 2011), suggesting that the effects of these mutations are more complex than initially thought.

The data presented here for Rag23, however, show that it is possible to have very high levels of agonist-induced activity and high ligand-binding affinity even when constitutive activity has been abolished. Analysis of the Rag23-A208L construct shows that this mutant also exhibits no constitutive activity, indicating reversion to L208 alone is not enough to restore constitutive activity. The fact that the Rag23-A208L mutant exhibits maximal NECA-induced activity similar to WT receptor suggests that the loss of constitutive activity observed is not due to a reduction in G-protein coupling. This was supported by radioligand-binding analysis performed with [$^3$H] NECA, which showed that the affinities of both the WT and Rag23-A208L are reduced by the same amount in the absence of G-protein. This is an important finding in view of the known effects of G-protein interactions on GPCR agonist affinities, and would be difficult to achieve in mammalian cells, which contain undefined G-protein species that can not be selectively removed. Previous analysis of the thermostabilizing mutants has been largely carried out by radioligand binding to receptor expressed in *E. coli*. The data shown here reveal that assessing the effects on downstream signalling using a more informative eukaryotic cell system is also important.

Previous research on the 5-hydroxytryptamine-4 receptor ($5\text{-}HT_4R$) indicates roles for a threonine residue in TM3 (Thr104) and a tryptophan residue in TM6 (Trp272) in the formation of a so-called double toggle switch in stabilizing the constitutively active conformation of the receptor (Pellissier *et al.*, 2009). Mutation of the Thr104 to an Ala leads to a dramatic decrease in constitutive activity. A comparison of the primary sequences indicates that Thr88 of $A_{2A}R$ is equivalent to Thr104 of $5\text{-}HT_4R$. However, in the case of the $A_{2A}R$, mutation of Thr88 to an Ala has little effect on the constitutive activity but a dramatic effect on agonist-induced activity both for NECA and adenosine. In addition, the T88A mutation is not present in either the Rag23 or Rag23-A208L mutants, which also do not exhibit constitutive activity. Therefore, the loss of constitutive activity observed in the $A_{2A}R$ mutants must have a different mechanism than the one proposed for $5\text{-}HT_4R$. Both the Rag23 and the Rant mutants exhibit a complete loss of constitutive activity but contain no common point mutations.

Of the individual point mutations generated, V239A exhibits maintained agonist-induced activity but a loss of constitutive activity. This residue is located on helix VI, pointing towards helices III and V. It is possible that the reduction in size of this residue by introduction of the Ala mutation allows helices III and VI to come into closer proximity and to form tighter interactions. These interactions may then prevent the movements of helices III and VI required for constitutive activation. Superposition of inactive $A_{2A}R$ structures (Figure 5) reveals that there is a 1.1 Å movement of helix III towards helix VI in an inactive thermostabilized mutant (containing the V239A mutation) structure (PDB: 3PWH) compared with the inactive $A_{2A}R$ bound to an antibody (PDB: 3VG9). This shift of helix III towards helix VI could explain the formation of the so-called ionic lock between the E/DRY motif and Glu228, which is not observed in the antibody-bound structure. The thermostabilized receptor contains other mutations but the only other one likely to play a role in this shift is the L235A, which is likely to have a

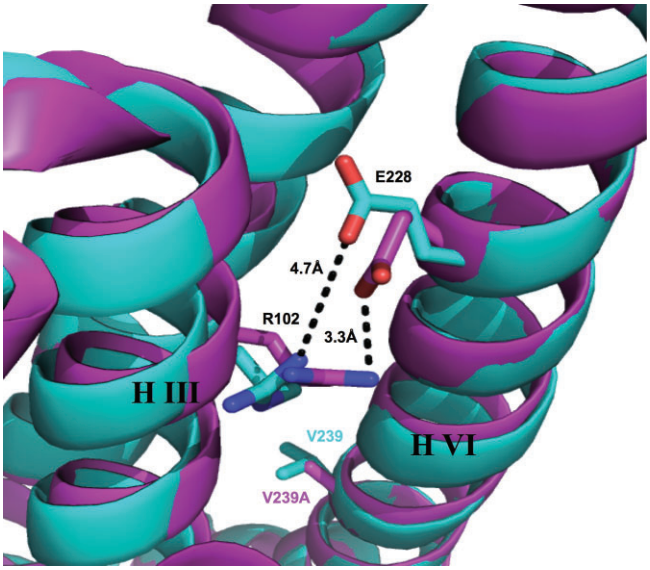


## Figure 5

Superposition of helices III and VI of the inactive thermostabilized $A_{2A}R$ mutant (containing the V239A mutation) structure (pink, Pdb accession code 3PWH) and the inactive $A_{2A}R$ bound to an antibody (blue Pdb, accession code 3VG9). The V239 or V239A and E228 residues located on helix VI and the R102 residue located on helix III are shown as stick models. The distance between the charged interacting groups of E228 and R102 of the ionic lock in each case are indicated by the dotted lines.

similar effect as the V239A. A potential caveat to this hypothesis is that the presence of the antibody may induce the differences observed between the two structures.

In summary, the use of the yeast cell growth assay has allowed a detailed analysis of the pharmacological effects of receptor mutations since it discriminates between constitutive and agonist-induced receptor signalling events. The data presented here also provide evidence that the agonist-induced and constitutively active conformations of the $A_{2A}R$ are distinct. This information is complementary to, and yet distinct from, that obtained from the recent high-resolution structures. Almost all of the GPCR structures obtained so far are of proteins, which have undergone significant modification, and the effects of this on coupling to the downstream signalling pathway have been largely ignored. The results of this study show the importance of assessing the effects of mutations on signalling as well as binding in order to gain a fuller understanding of the engineered protein structures. In order to fully understand the mechanism of action of GPCRs, it will be necessary to functionally and structurally characterize all the different active conformations. The research findings are strongly indicative that the yeast cell system is representative of lower throughput mammalian cell systems, making it useful for functional studies of mammalian receptors. However, future studies could focus on a detailed comparison of the two systems.

The data presented here coupled with the high-resolution structure information may form the basis of rational design of receptor-specific drugs that can antagonize constitutive activity with no effect on agonist-induced activity. In addition, this work suggests that increased receptor thermostability is correlated with the loss of constitutive activity. It may be that the yeast cell growth assay used in combination with either alanine-scanning mutagenesis or random mutagenesis methods (Dodevski and Plückthun, 2011) would provide a powerful screening tool for the production of thermostable mutants of other GPCRs. Furthermore, by using the yeast growth assay as an initial screen, it will be possible to select those mutants that retain some functionality.

## Acknowledgements

The authors wish to thank Dr David Grose, Dr Ashley Barnes, and Dr Andrew Brown for advice on the yeast functional assay and for helpful discussions, and Dr Mike Hann, Dr Kate Smith, Dr Danuta Mossakowska and Dr Minghao Zhang for helpful discussions. We are particularly grateful to Prof Philip Strange for his insights into models of GPCR activation.

## Conflict of interest

None.

## References

Alexander SP, Millns PJ (2001). [(3)H]ZM241385 – an antagonist radioligand for adenosine A(2A) receptors in rat brain. Eur J Pharmacol 411: 205–210.

Brown AJ, Goldsworthy SM, Barnes AA, Eilert MM, Tcheang L, Daniels D *et al.* (2003). The Orphan G protein-coupled receptors GPR41 and GPR43 are activated by propionate and other short chain carboxylic acids. J Biol Chem 278: 11312–11319.

Cherezov V, Rosenbaum DM, Hanson MA, Rasmussen SGF, Thian FS, Kobilka TS *et al.* (2007). High-resolution crystal structure of an engineered human beta2-adrenergic G protein-coupled receptor. Science 318: 1258–1265.

Chien EYT, Liu W, Zhao Q, Katritch V, Han GW, Hanson MA *et al.* (2010). Structure of the human dopamine D3 receptor in complex with a D2/D3 selective antagonist. Science 330: 1091–1095.

Dodevski I, Plückthun A (2011). Evolution of three human GPCRs for higher expression and stability. J Mol Biol 408: 599–615.

Doré AS, Robertson N, Errey JC, Ng I, Hollenstein K, Tehan B *et al.* (2011). Structure of the adenosine A(2A) receptor in complex with ZM241385 and the xanthines XAC and caffeine. Structure 19: 1283–1293.

Dowell SJ, Brown AJ (2009). Yeast assays for G protein-coupled receptors. Methods Mol Biol 552: 213–229.

Drew D, Newstead S, Sonoda Y, Kim H, Heijne von G, Iwata S (2008). GFP-based optimization scheme for the overexpression and purification of eukaryotic membrane proteins in *Saccharomyces cerevisiae*. Nat Protoc 3: 784–798.

Gietz RD, Schiestl RH (2007). High-efficiency yeast transformation using the LiAc/SS carrier DNA/PEG method. Nat Protoc 2: 31–34.

Gloriam DE, Fredriksson R, Schiöth HB (2007). The G protein-coupled receptor subset of the rat genome. BMC Genomics 8: 338.

Granier S, Manglik A, Kruse AC, Kobilka TS, Thian FS, Weis WI *et al.* (2012). Structure of the δ-opioid receptor bound to naltrindole. Nature 485: 400–404.

Jaakola V-P, Griffith MT, Hanson MA, Cherezov V, Chien EYT, Lane JR *et al.* (2008). The 2.6 angstrom crystal structure of a human A2A adenosine receptor bound to an antagonist. Science 322: 1211–1217.

Jiang Q, Van Rhee AM, Kim J, Yehle S, Wess J, Jacobson KA (1996). Hydrophilic side chains in the third and seventh transmembrane helical domains of human A2A adenosine receptors are required for ligand recognition. Mol Pharmacol 50: 512–521.

Klinger M, Kuhn M, Just H, Stefan E, Palmer T, Freissmuth M *et al.* (2002). Removal of the carboxy terminus of the A2A-adenosine receptor blunts constitutive activity: differential effect on cAMP accumulation and MAP kinase stimulation. Naunyn Schmiedebergs Arch Pharmacol 366: 287–298.

Kobilka BK, Deupi X (2007). Conformational complexity of G-protein-coupled receptors. Trends Pharmacol Sci 28: 397–406.

Lebon G, Warne T, Edwards PC, Bennett K, Langmead CJ, Leslie AGW *et al.* (2011). Agonist-bound adenosine A(2A) receptor structures reveal common features of GPCR activation. Nature 474: 521–525.

Magnani F, Shibata Y, Serrano-Vega MJ, Tate CG (2008). Co-evolving stability and conformational homogeneity of the human adenosine A2a receptor. Proc Natl Acad Sci U S A 105: 10744–10749.

Milligan G, Bond RA, Lee M (1995). Inverse agonism: pharmacological curiosity or potential therapeutic strategy? Trends Pharmacol Sci 16: 10–13.

Newstead S, Kim H, von Heijne G, Iwata S, Drew D (2007). High-throughput fluorescent-based optimization of eukaryotic membrane protein overexpression and purification in *Saccharomyces cerevisiae*. Proc Natl Acad Sci U S A 104: 13936–13941.

O'Malley MA, Lazarova T, Britton ZT, Robinson AS (2007). High-level expression in *Saccharomyces cerevisiae* enables isolation and spectroscopic characterization of functional human adenosine A2a receptor. J Struct Biol 159: 166–178.

Olesnicky NS, Brown AJ, Dowell SJ, Casselton LA (1999). A constitutively active G-protein-coupled receptor causes mating self-compatibility in the mushroom Coprinus. EMBO J 18: 2756–2763.

Peeters MC, van Westen GJP, Li Q, Ijzerman AP (2011). Importance of the extracellular loops in G protein-coupled receptors for ligand recognition and receptor activation. Trends Pharmacol Sci 32: 35–42.

Pellissier LP, Sallander J, Campillo M, Gaven F, Queffeulou E, Pillot M *et al.* (2009). Conformational toggle switches implicated in basal constitutive and agonist-induced activated states of 5-hydroxytryptamine-4 receptors. Mol Pharmacol 75: 982–990.

Rasmussen SGF, Devree BT, Zou Y, Kruse AC, Chung KY, Kobilka TS *et al.* (2011). Crystal structure of the β2 adrenergic receptor-Gs protein complex. Nature 477: 549–555.

Serrano-Vega MJ, Tate CG (2009). Transferability of thermostabilizing mutations between beta-adrenergic receptors. Mol Membr Biol 26: 385–396.

Serrano-Vega MJ, Magnani F, Shibata Y, Tate CG (2008). Conformational thermostabilization of the beta1-adrenergic receptor in a detergent-resistant form. Proc Natl Acad Sci U S A 105: 877–882.

Shibata Y, White JF, Serrano-Vega MJ, Magnani F, Aloia AL, Grisshammer R *et al.* (2009). Thermostabilization of the neurotensin receptor NTS1. J Mol Biol 390: 262–277.

Shimamura T, Shiroishi M, Weyand S, Tsujimoto H, Winter G, Katritch V *et al.* (2011). Structure of the human histamine H1 receptor complex with doxepin. Nature 475: 65–70.

Singh S, Gras A, Fiez-Vandal C, Ruprecht J, Rana R, Martinez M *et al.* (2008). Large-scale functional expression of WT and truncated human adenosine A2A receptor in Pichia pastoris bioreactor cultures. Microb Cell Fact 7: 28.

Singh S, Hedley D, Kara E, Gras A, Iwata S, Ruprecht J *et al.* (2010). A purified C-terminally truncated human adenosine A(2A) receptor construct is functionally stable and degradation resistant. Prot Express Purif 74: 80–87.

Strange PG (2002). Mechanisms of inverse agonism at G-protein-coupled receptors. Trends Pharmacol Sci 23: 89–95.

Thompson AA, Liu W, Chun E, Katritch V, Wu H, Vardy E *et al.* (2012). Structure of the nociceptin/orphanin FQ receptor in complex with a peptide mimetic. Nature 485: 395–399.

Uustare A, Vonk A, Terasmaa A, Fuxe K, Rinken A (2005). Kinetic and functional properties of [3H]ZM241385, a high affinity antagonist for adenosine A2A receptors. Life Sci 76: 1513–1526.

Warne T, Serrano-Vega MJ, Baker JG, Moukhametzianov R, Edwards PC, Henderson R *et al.* (2008). Structure of a beta1-adrenergic G-protein-coupled receptor. Nature 454: 486–491.

Warne T, Moukhametzianov R, Baker JG, Nehmé R, Edwards PC, Leslie AGW *et al.* (2011). The structural basis for agonist and partial agonist action on a β(1)-adrenergic receptor. Nature 469: 241–244.

Wu B, Chien EYT, Mol CD, Fenalti G, Liu W, Katritch V *et al.* (2010). Structures of the CXCR4 chemokine GPCR with small-molecule and cyclic peptide antagonists. Science 330: 1066–1071.

Wu H, Wacker D, Mileni M, Katritch V, Han GW, Vardy E *et al.* (2012). Structure of the human κ-opioid receptor in complex with JDTic. Nature 485: 327–332.

Xu F, Wu H, Katritch V, Han GW, Jacobson KA, Gao Z-G *et al.* (2011). Structure of an agonist-bound human A2A adenosine receptor. Science 332: 322–327.

## Supporting information

Additional Supporting Information may be found in the online version of this article at the publisher's web-site:

**Figure S1** (A) NECA-induced activity of the WT $A_{2A}R$ in the presence of a range of different 3AT concentrations. The receptor was expressed in the MMY24 *Saccharomyces cerevisiae* strain as a construct in the p306GPD vector. (B) Receptor activation of both WT receptor and an empty vector control at the optimal concentration of 3AT (5 mM) as determined in A.

**Figure S2** Activity of the WT $A_{2A}R$ in the presence of a range of different concentrations of an agonist (NECA), and two inverse agonists GW866133X and GSK124631A with pIC50s of 9.0 and 8.4 respectively. A neutral compound with no

effect on $A_{2A}R$ activity, HU210, a CB1 agonist was also added as a control. The receptor was expressed in the MMY24 *Saccharomyces cerevisiae* strain as a construct in the p306GPD vector.

**Table S1** Mutagenic primers used to generate the single and double mutant $A_{2A}R$ constructs.

**Table S2** Expression levels of the different $A_{2A}R$ + GFP constructs in the MMY24 strain. The expression levels of all constructs were calculated from the relative fluorescence units as described in Drew *et al*. (2008). The $B_{max}$ values of the WT, Rant and Rag constructs were assessed by radioligand-binding analysis of membrane bound receptor.